

# Spikiness Assessment of Term Occurrences in Microblogs: an Approach Based on Computational Stigmergy

Mario G.C.A. Cimino<sup>1</sup>, Federico Galatolo<sup>1</sup>, Alessandro Lazzeri<sup>1</sup>,  
Witold Pedrycz<sup>2</sup>, and Gigliola Vaglini<sup>1</sup>

<sup>1</sup>Department of Information Engineering, University of Pisa, Largo Lazzarino 1, Pisa, Italy

<sup>2</sup>Department of Electrical and Computer Engineering, University of Alberta, Edmonton, T6R 2V4 AB, Canada  
[mario.cimino@unipi.it](mailto:mario.cimino@unipi.it), [f.galatolo1@studenti.unipi.it](mailto:f.galatolo1@studenti.unipi.it), [alessandro.lazzeri@for.unipi.it](mailto:alessandro.lazzeri@for.unipi.it),  
[wpedrycz@ualberta.ca](mailto:wpedrycz@ualberta.ca), [gigliola.vaglini@unipi.it](mailto:gigliola.vaglini@unipi.it)

**Keywords:** Microblog Analytics, Spikiness Assessment, Computational Stigmergy, Term Cloud.

**Abstract:** A significant phenomenon in microblogging is that certain occurrences of terms self-produce increasing mentions in the unfolding event. In contrast, other terms manifest a spike for each moment of interest, resulting in a wake-up-and-sleep dynamic. Since spike morphology and background vary widely between events, to detect spikes in microblogs is a challenge. Another way is to detect the spikiness feature rather than spikes. We present an approach which detects and aggregates spikiness contributions by combination of spike patterns, called archetypes. The soft similarity between each archetype and the time series of term occurrences is based on computational stigmergy, a bio-inspired scalar and temporal aggregation of samples. Archetypes are arranged into an architectural module called Stigmergic Receptive Field (SRF). The final spikiness indicator is computed through linear combination of SRFs, whose weights are determined with the Least Square Error minimization on a spikiness training set. The structural parameters of the SRFs are instead determined with the Differential Evolution algorithm, minimizing the error on a training set of archetypal series. Experimental studies have generated a spikiness indicator in a real-world scenario. The indicator has enhanced a cloud representation of social discussion topics, where the more spiky cloud terms are more blurred.

## 1 INTRODUCTION

Microblogging systems are increasingly used in the everyday life, producing in real time a huge amount of informal and unstructured messages. In the literature, a research challenge is to identify and separate the temporal dynamics of a specific event, summarizing or visualizing such information in order to make it accessible to human analysts. A relevant dynamic is that certain occurrences of terms self-produce increasing mentions in the unfolding event, whereas other terms manifest a *spike* for each moment of interest, resulting in a wake-up-and-sleep pattern called *spikiness* (Gruhl & Guha, 2004), (Highfield *et al.*, 2013).

Automatic spike detection on Microblogs is a difficult task, because: (i) experts usually provide simplistic spike definitions; (ii) two human experts often do not mark the same events as spikes; (iii) the ratio of candidate spike events to actual spike events is large; (iv) spike morphology and background vary

widely between events; (v) well defined training set are time consuming and expensive to develop.

As an example, Fig. 1 shows the dynamics of some major terms used on Twitter during the terrorist attack in Paris on 13 Nov 2015, by gunmen and suicide bombers. In particular, Fig. 1a-c show different spike morphologies and durations: *thought* (short duration), *killed* (medium duration), and *terrorism* (long duration). Fig. 1d-e show different spikiness degrees: *terrorist attack* (low spikiness) and *police* (high spikiness).

In the literature, many statistical and machine learning techniques have been used for the automatic spike detection (Yun, 2011), (Marcus *et al.*, 2011), (Nichols *et al.*, 2012), (Lehmann *et al.*, 2012), (Birdsey *et al.*, 2015). In this paper we present an innovative technique based on computational stigmergy (Avvenuti, 2013), (Barsocchi, 2015), a bio-inspired paradigm of emergent systems. In the literature, a well-known form of stigmergy is

manifested by by societies of insects (Dorigo *et al.* 2000), (Mohan *et al.* 2012).

In the basic mechanism of stigmergic computing each sample of a time series releases a *mark* (i.e. a digital pheromone) in the scalar space, evaporating over time. As a result, marks with scalar and temporal proximity overlap, generating functional structures called *trails*. A trail enables a short-term and short-size granulation mechanism, appearing and staying spontaneous at runtime when local dynamics in samples occurs. A similarity operator is used to associate the dynamic of a sequence of samples against a collection of predefined sequences called archetypes.

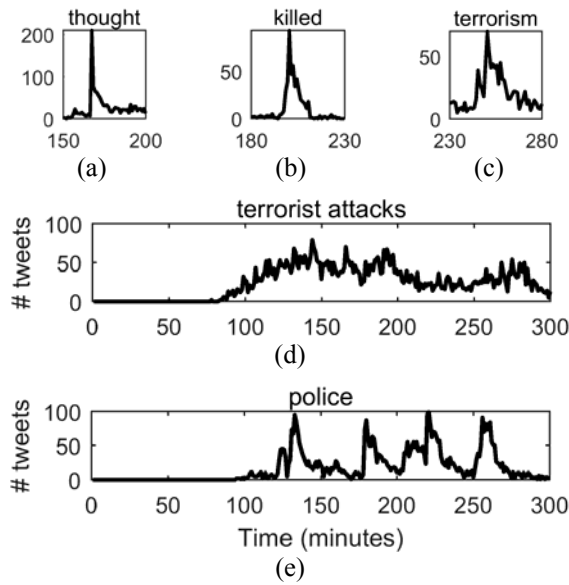


Figure 1: Three spikes morphologies and durations: (a) short spike duration, (b) medium spike duration, (c) long spike duration. Two spikiness degrees: (d) low spikiness, (e) high spikiness.

The computational unit of our architecture is called *Stigmergic Receptive Field* (SRF) (Cimino *et al.* 2006). We use SRFs to detect the spikiness of time series generated by event-specific terms. In a SRF, the spikiness feature is modeled by a collection of archetypal spikes with different morphologies. The training of a SRF consists in optimizing its parameters via the Differential Evolution algorithm (Cimino *et al.* 2015), (Alfeo *et al.*, 2016). The SRF compares the stigmergic trail released by an archetypal spike with the stigmergic trail of the current time series, and provides the measure of similarity. To combine the different spikiness morphology represented by the different archetypal spikes, the SRFs are arranged in a Stigmergic

Perceptron (SP). Since the SP manages archetypal spikes of a specific scale, multiple SPs have been used to identify different sized spikiness. Finally, the spikiness indicator is generated through a linear combination of SRFs, whose weights are calculated by means of the Least Square Error minimization on some desired spikiness provided by human experts.

The paper is structured as follow: Section 2 summarizes the related works on spike detection in Microblogs. Section 3 comprises the design of the functional modules of our approach. Section 4 covers the experimental studies. Finally, Section 5 draws conclusions and future work.

## 2 RELATED WORK

Several authors studied the dynamics of temporal usage of terms in Microblogs, using distance measures for time series (Fu 2011), (Esling *et al.*, 2012). Gruhl & Guha (2004) present three main types of topics pattern on blogs: (i) *just spike*: topics which at some point switch from inactive to very active, and then back to inactive; (ii) *spiky chatter*: topics with a significant chatter level, very sensitive to external world events; (iii) *mostly chatter*, topics continuously discussed at relatively moderate levels. Highfield *et al.* (2013) examine the use of Twitter for the expression of shared fandom in the context of the Eurovision Song Contest. The authors found that the presence of a spike is usually related to particular event occurred during the show.

Yun (2011) distinguishes between three types of topic: *peaky topics*, *constant topics* and *regularly repeated topics*. The author defines specific criteria and uses statistical methods to differentiate the three categories. Marcus *et al.* (2011) identify spikes in a temporal collection of tweet, by computing the average rate of messages in a sliding window. More precisely, a spike is found when the rate in a window is a local maximum, i.e. the side windows have lower rates. Nichols *et al.* (2012) present an algorithm for spike detection used to summarize sporting events from Twitter messages. The algorithm is based on the change in the volume of the published tweet per minute according to a slope threshold. The threshold is computed for the entire event from basic statistics of the set of all slopes for that event. Similarly, Lehmann *et al.*, (2012) study the daily evolution of hashtags popularity over multiple days, considering one hour as a time unit. The identification of an activity peak is based on the change in the volume according to a statistical baseline and a tunable threshold. They identify four

different categories of spike-shaped temporal patterns, depending on the concentration around the event: *before and during the event*, *during and after the event*, *symmetrically around the event*, and *only during the event*. Birdsey *et al.* (2015) propose an approach based on four state of a topic: *rising*, *plateau*, *burst*, and *stabilization*. To identify the state the authors define a metric named intensity, which is directly proportional to the number of messages related to the topic and the number of total users (publishers), and inversely proportional to the total number of messages and the number of unique user posting on the topic. According to a threshold and the metric, the topic switches from a state to another.

### 3 FUNCTIONAL DESIGN

This Section formally introduces the major functional components of our algorithm.

#### 3.1 The Stigmergic Receptive Field

Let  $\ddot{d}(k)$  denote the values of a time series at discrete-time  $k$ . A linear transformation of the time series called *min-max normalization* is assumed:

$$d(k) = \text{MinMaxNorm}(\ddot{d}(k)) \triangleq \frac{\ddot{d}(k) - \ddot{d}_{\text{MIN}}}{\ddot{d}_{\text{MAX}} - \ddot{d}_{\text{MIN}}} \quad (1)$$

which is a linear mapping of the data samples in the interval  $[0,1]$ , where the bounds  $\ddot{d}_{\text{MIN}}$  and  $\ddot{d}_{\text{MAX}}$  are estimated in an observation time window. To assure samples are positioned between 0 and 1, the results are clipped to  $[0,1]$ .

Normalized data samples are processed by *clumping*, in which samples of a particular range group close to one another. Clumping is a kind of parametric soft discretization of the continuous-valued samples to a set of levels:

$$d_c(k) \equiv \text{Clumping}(d(k); \alpha_c, \beta_c) \triangleq \begin{cases} 0, & d(k) \leq \alpha_c \\ 2 \left( \frac{d(k) - \alpha_c}{\beta_c - \alpha_c} \right)^2, & \alpha_c < d(k) \leq \frac{\alpha_c + \beta_c}{2} \\ 1 - 2 \left( \frac{d(k) - \beta_c}{\beta_c - \alpha_c} \right)^2, & \frac{\alpha_c + \beta_c}{2} < d(k) < \beta_c \\ 1, & d(k) \geq \beta_c \end{cases} \quad (2)$$

As an implementation of clumping, we adopt the *s-shaped* function, shown in Fig. 2a. Given  $\alpha_c, \beta_c \in (0,1)$  input values smaller | larger than  $(\beta_c$

$-\alpha_c)/2$  are lowered | raised; values smaller | larger than  $\alpha_c$  |  $\beta_c$  assume the minimum | maximum value, i.e.,  $0|1$ . Fig. 2b shows an example of series, in dotted line, and the effect of the clumping, in solid line.

Clumped data samples are processed by *marking*, in which each sample produces a corresponding *mark*:

$$M(k) \equiv \text{Marking}(d_c(k); \varepsilon_1, \varepsilon_2) \quad (3)$$

As an implementation of marking, we adopt the *trapezoid* function, shown in Fig. 3, defined by the center  $d_c(k)$ , a fixed height equals to 1, upper and lower-bases,  $\varepsilon_1$  and  $\varepsilon_2$ . Since the ratio  $\varepsilon_1/\varepsilon_2$  is statically prefixed to  $2/3$ , we can refer to the mark as  $\text{Marking}(d_c(k); \varepsilon)$ .

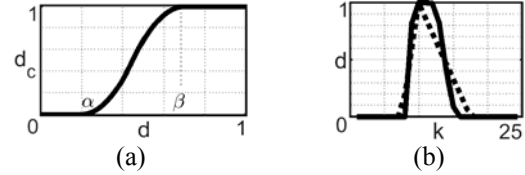


Figure 2: The s-shaped function with  $\alpha_c = 0.22$  and  $\beta_c = 0.76$  (a), and the clumping (solid) of the input series (dotted).

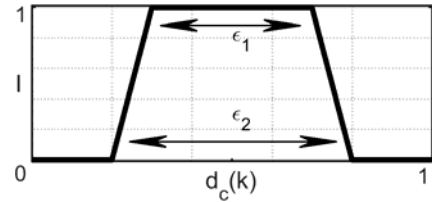


Figure 3: The trapezoidal mark, centered in  $d_c = 0.5$ , with  $\varepsilon_1 = 0.4$  and  $\varepsilon_2 = 0.6$ .

With the *trailing*, the evaporation and the accumulation of the marks over time create the *trail* structure:

$$T(k) \equiv \text{Trailing}(T(k-1), M(k); \delta) \quad (4)$$

$$T'(k) = \begin{cases} 0, & \text{if } T(k-1) \leq \delta \\ T(k-1) - \delta, & \text{otherwise} \end{cases} \quad (5)$$

$$T(k) = T'(k) + M(k) \quad (6)$$

The evaporation is regulated by the rate  $0 \leq \delta < 1$ . Fig. 4a and Fig. 4a show the release of a mark with  $\varepsilon_2 = 0.24$  on  $d_c(0) = 0$ , and the trail after the evaporation with  $\delta = 0.34$  and the release of the second mark on  $d_c(1) = 0$ .

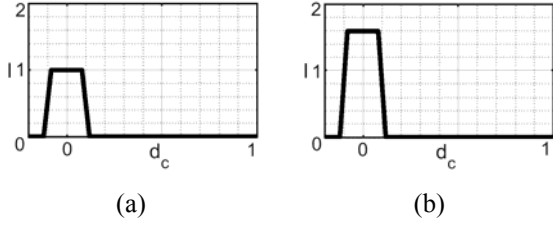


Figure 4: (a) The release of a mark with  $\varepsilon_2 = 0.24$  on  $d_c(0) = 0$ ; (b) The trail after the evaporation with  $\delta = 0.34$  and the release of the second mark on  $d_c(1) = 0$ .

As a consequence, an isolated mark tends to disappear from the trail, reducing the influence of spurious samples in the temporal pattern. In contrast, subsequent marks sum their intensities if superimposed with other marks generating a more persistent structure.

A *Stigmergic Receptive Field* (SRF) is fed by two time series, i.e.,  $d(k)$  and  $\bar{d}(k)$ . Given a sliding time window, of size  $N$ , it takes two parallel segments  $\{d(k)\}_{|_N} \equiv \{d(k_1), \dots, d(k_N)\}$   $\{\bar{d}(k)\}_{|_N} \equiv \{\bar{d}(k_1), \dots, \bar{d}(k_N)\}$ , and returns the activation  $a(h) \in [0, 1]$ , which is close to 0 | 1 if the two segments are dissimilar | similar. As an example Fig. 5 shows two input parallel segments, with  $N=25$ .

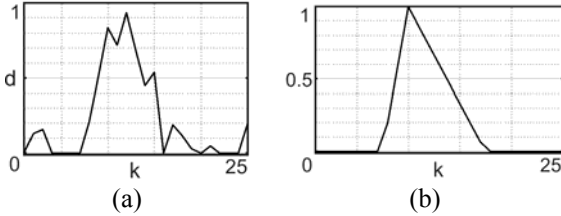


Figure 5: Two input segments (a)  $\{d(k)\}$  and (b)  $\{\bar{d}(k)\}$  of a Stigmergic Receptive Field.

In a SRF, the two segments are processed in parallel, by means of clumping, marking and trailing, thus generating two corresponding trails  $T(k)$  and  $\bar{T}(k)$ . Subsequently, the *similarity* between the two trails is computed:

$$s(h) \equiv \text{Similarity}(T(k), \bar{T}(k)) \in [0, 1] \quad (7)$$

As an implementation of similarity, we adopt the Jaccard's coefficient, which is the ratio between the intersection and the union of the trails:

$$s(h) \triangleq T(k) \cap \bar{T}(k) / T(k) \cup \bar{T}(k) \quad (8)$$

As an example, Fig. 6 shows two trails (in solid and dotted line), the intersection (dark gray), and the union as the area covered by the light gray, dark gray, and the white areas underlying the trails.

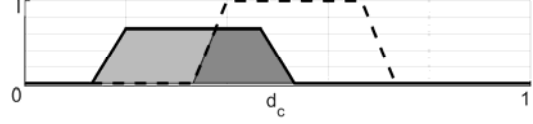


Figure 6: Representation of the intersection and union between two trails.

We remark that for each pair of segment, each made by  $N$  samples, a single similarity sample  $s(h)$  is released, i.e.  $N = k/h$ ,  $N \gg 1$ .

Finally, the *activation* of the similarity sample is computed:

$$a(h) \equiv \text{Activation}(s(h); \alpha_A, \beta_A) \quad (9)$$

As an implementation of activation, we adopt the *s-shaped* function. The activation increases | decreases the rate of similarity potential firing the SRF. The term “activation” is borrowed from neural sciences: it inhibits low intensity signals while boosts signals reaching a certain level to enable the next layer of processing (Cimino, 2009).

We remark that, although the clumping and the activation are implemented by the same function, their meaning is very different. Indeed, in contrast to the activation, the clumping may be implemented by a multi-level s-shape function, when different levels of interest are comprised in the input space.

### 3.2 The Adaptation of the SRF

The SRF should be properly parameterized to enable an effective aggregation of input samples and output activation:

$$a(h) = \text{SRF}\left(\{d(k)\}_{|_N}, \{\bar{d}(k)\}_{|_N}; \alpha_c, \beta_c, \varepsilon, \delta, \alpha_A, \beta_A\right) \quad (10)$$

For example, short-life marks evaporate too fast, preventing aggregation and pattern reinforcement, whereas long-life marks cause early activation.

The *adaptation* is an offline function, taking as an input a SRF and a tuning set made by a set  $Z$  of *(input, desired output)* pairs. As an output, the adaptation provides a set of structural parameters of the SRF:

$$\begin{aligned} &\text{Adaptation}\left(\text{SRF}, \left\{\{d(k^*), \bar{d}(k^*)\}_{|_N}, a(h^*)\right\}\right) \\ &= \{\alpha_c, \beta_c, \varepsilon, \delta, \alpha_A, \beta_A\} \end{aligned} \quad (11)$$

As an implementation of adaptation, we use the Differential Evolution algorithm. In (Cimino, 2015), the authors carry out a comparative study of three evolutionary algorithms: Particle Swarm Optimization, Genetic Algorithm, and Differential Evolution. As a result, the latter shows better performance both in speed and quality of the solution. The fitness function is the Mean Squared Error (MSE) between the output  $SRF'$  provided for a certain input and the desired output  $SRF$  provided in the tuning set for the same input:

$$f(Z) = \frac{1}{|Z|} \sum_z (SRF_z - SRF'_z)^2 \quad (12)$$

The objective is to train the SRF to accurately recognize the (dis-)similarity between segments.

### 3.3 The Stigmergic Perceptron

A single SRF can be used to recognize the (dis-)similarity between a time series and an *archetypal* time series, which represents a pattern. In the spikiness domain, we can have more than one archetype. Fig.7 shows three spikiness archetypes in a time window. Here, the different positions of the archetypes represent an early, a timely, and a late spike. This allows identifying the spike independently on the temporal shift with respect to the time window.

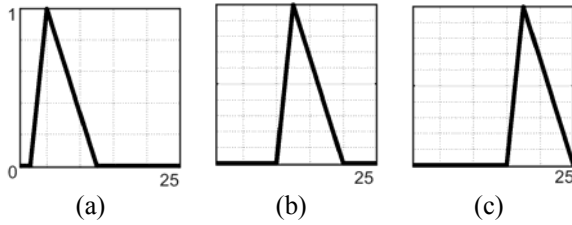


Figure 7: Spikiness archetypes: (a) early spike; (b) timely spike; (c) late spike.

A *Stigmergic Perceptron* takes as an input the output of each SRF, one per each archetype, and provides the output of the SRF with the best activation:

$$g(h) \equiv SP[\{SRF(h)\}] \quad (13)$$

As an implementation of the SP, we use the maximum between the activations:

$$g(h) \triangleq \max_{SRF} \{a_{SRF}(h)\} \quad (14)$$

### 3.4 The Spikiness Information Fusion

The assessment of the spikiness level of the overall series is based on the aggregation of three different Stigmergic Perceptrons. Each SP employs different archetypes: short spike duration, medium spike duration, and long spike duration. The assessment is based on a number of  $U$  non-overlapping time windows, for each SP. The outputs of each SP are summated:

$$A_i = \sum_{u=1}^U SP_i(h_u) \quad (15)$$

Given that there are no dependencies between the processing of each SP, the values of  $A_i$  can be computed in parallel.

Finally, the activation values  $A_k$  are aggregated by means of a weighted sum to generate the spikiness level:

$$S_{LEVEL} \equiv SIF(\{A_i\}; \{w_i\}) \triangleq \sum_{i=1}^3 A_i * w_i \quad (16)$$

the weights  $w_i$  are determined through a standard Least Square Error optimization, which minimizes the error with respect to a set of spikiness level generated by human observation:

$$\text{Optimization}(\{SP\}, \{S_{LEVEL}^*\}) = \{w_i\} \quad (17)$$

It follows (Algorithm 1) the overall algorithm for the calculation of the spikiness level of a set of given time series  $\{D\}$ .

## 4 EXPERIMENTAL STUDIES

To study the effectiveness of the algorithm, we have analyzed a dataset of 188,607 Twitter posts collected during the terrorist attacks in Paris on November 13, 2015, between 9 PM of November 13 and 2 AM of November 14.

The dataset was first pre-processed by removing stop words, i.e., common words used in a language. We also removed the historical baseline, i.e., a set of terms generally related to the class of the event rather than to its specific occurrence. Subsequently, the most frequent 100 terms were selected, and the corresponding time series were generated using a time windows of 1 minute.

The time series were annotated by a group of four human annotators, who assigned two different indicators to each series:

- (i) *spikiness level*: it is an integer ranging from 0 (no-spikiness) to 4 (maximum-spikiness). As an example, the series of Fig.1d and Fig.1e have spikiness levels 1 and 4, respectively. In general, the spikiness level is proportional to the number of occurrences of the wake-up-and-sleep

dynamic. The spikiness level is then normalized dividing by 4.

- (ii) *spikiness dimension*: it is the characterization of the overall durations of spikes. Let us assume the three types of spike represented in Fig.1 a-c, with an order: 1: *short*, 2: *medium*, 3: *high*. Let us consider the series of Fig.1e: since the medium duration is the most frequent, and the short duration is less frequent, the spikiness dimension is 2|3|1. Considering Fig.1d, the short duration is the most frequent, and the long duration is the less frequent. Thus, the spikiness dimension is 1|2|3. Actually, the most wake-up-and-sleep dynamics are not complete in Fig.1e, but our focus is on spikiness rather than on spikes.

---

**Algorithm 1: Spikiness ( $\{\tilde{D}\}$ )**

---

```

 $D \leftarrow \text{MinMaxNorm}(\tilde{D})$ 
Adaptation( $\{SRF, \{d(k^*), \bar{d}(k^*)\}_N, a(h^*)\}$ )
=  $\{\alpha_c, \beta_c, \varepsilon, \delta, \alpha_a, \beta_a\}$ 
Optimization( $\{SP\}, \{S_{LEVEL}^*\}$ ) =  $\{w_i\}$ 
par for each  $d$  in  $\{D\}$ 
  par for each  $i$  in  $\{SP\}$ 
    par for each time window  $h$ 
      for each instant  $k$ 
         $d_c(k) \equiv \text{Clumping}(d(k); \alpha_c, \beta_c)$ 
         $M(k) \equiv \text{Marking}(d_c(k); \varepsilon)$ 
         $T(k) \equiv \text{Trailing}(T(k-1), M(k); \delta)$ 
      end for
       $s(h) \equiv \text{Similarity}(T(k), \bar{T})$ 
       $a(h) \equiv \text{Activation}(s(h); \alpha_a, \beta_a)$ 
       $g(h) \equiv \text{SP}[\{SRF(h)\}]$ 
    end for
     $A_i = \sum_{u=1}^U SP_i(h_u)$ 
  end for
end for
 $S_{LEVEL} \equiv \text{SIF}(\{A_i\}; \{w_i\})$ 
return  $S_{LEVEL}$ 

```

---

Each annotator observed all the time series to have an overview of the temporal patterns. Finally, the annotators achieved consensus providing the indicators for each time series.

Table 1 shows the confusion matrix of the human classification compared with the same output provided by the system. We remark that the 86% of the time series are correctly identified by the system

(diagonal values, represented in boldface). A significant number of misclassification is between the dimensions 2|1|3 and 1|2|3, which means that some spikes with short and medium duration are inversely ranked.

The evaluation of the error on spikiness level is calculated with a 5-fold cross-validation: we divided our dataset into five randomly generated and equally-sized folds. Then, we used each fold as a test set and the remaining folds as a training set. Finally, we calculated the average MSE  $\pm$  standard deviation, as shown in Table 2. We remark that the MSE on the training and test sets are very similar, thus confirming the good generalization of the system. We also remark that MSE is less than half of the difference between two spikiness levels ( $1/4 = 0.25$ ), thus confirming a good accuracy. Finally, the standard deviation is more than an order of magnitude lower than the MSE, thus showing a good precision.

Table 1: Confusion matrix of the spikiness dimension.

		System					
		1 2 3	1 3 2	2 1 3	2 3 1	3 1 2	3 2 1
Human	1 2 3	<b>21</b>	0	4	0	0	0
	1 3 2	0	<b>4</b>	2	0	0	0
	2 1 3	2	0	<b>53</b>	1	0	0
	2 3 1	1	0	3	<b>7</b>	0	0
	3 1 2	0	0	0	0	<b>1</b>	1
	3 2 1	0	0	0	0	0	<b>0</b>

Table 2: Fitness of the 5-Fold Cross Validation.

MSE (mean $\pm$ standard deviation)	
Training Set	Test Set
0.1146 $\pm$ 0.0037	0.1197 $\pm$ 0.0184

As a final result, the spikiness level has been used to enrich the term cloud representing the content of the discussion topics of a given event. Fig.8 shows an excerpt of a term cloud with a blur proportional to the spikiness level. Here, it is apparent that even large terms can have a high spikiness level, and those terms without spikiness are clearly discerned.

## 5 CONCLUSIONS

This paper presents an innovative computational technique for assessing the spikiness of terms in microblogs. The core processing is based on

computational stigmergy, a bio-inspired mechanism for scalar and temporal processing of time series. Experimental results have shown a very high number of correctly detected spikiness dimension, and a very low error on spikiness level for training and testing sets. The spikiness indicator has been visualized in a term cloud as a blur effect, making it apparent. To conduct performance evaluations on other datasets as well as comparative analyses with other approaches is considered a key investigation activity for future work.



Figure 8: An excerpt of the term cloud with blur proportional to the spikiness level.

## ACKNOWLEDGEMENTS

This work was partially supported by the PRA 2016 project “Analysis of Sensory Data: from Traditional Sensors to Social Sensors” funded by the University of Pisa.

## REFERENCES

- Alfeo, A. L., Appio, F. P., Cimino, M. G., Lazzeri, A., Martini, A., & Vaglini, G., 2016. An Adaptive Stigmergy-based System for Evaluating Technological Indicator Dynamics in the Context of Smart Specialization. In *ICPRAM 2016, 5th International Conference on Pattern Recognition Applications and Methods*, INSTICC, pp. 497-502.
- Avvenuti, M., Cesarini, D., Cimino, M.G.C.A., 2013. MARS, a multi-agent system for assessing rowers' coordination via motion-based stigmergy. *Sensors*, MDPI, 13(9), 12218-12243.
- Gruhl, D., Guha, R., 2004. Information Diffusion Through Blogspace. In *WWW'04, 13th International World Wide Web Conference*, pp. 491-501.
- Highfield, T., Harrington, S., Bruns, A., 2013. Twitter as a technology for audiencing and fandom. *Information, Communication & Society*, Taylor & Francis, 16(3), 315-339.
- Barsocchi, P., Cimino, M.G.C.A., Ferro, E., Lazzeri, A., Palumbo, F., Vaglini, G., 2015. Monitoring elderly behavior via indoor position-based stigmergy. *Pervasive and Mobile Computing*, Elsevier Science, 23, 26-42.
- Birdsey, L., Szabo, C., Teo, Y. M., 2015. Twitter knows: understanding the emergence of topics in social networks. In *WSC 2015, the 2015 Winter Simulation Conference*, IEEE, pp. 4009-4020.
- Cimino, M.G.C.A., Pedrycz, W., Lazzerini, B., Marcelloni, F., 2009. Using Multilayer Perceptrons as Receptive Fields in the Design of Neural Networks. *Neurocomputing*, Elsevier Science, 72(10-12), 2536-2548.
- Cimino, M.G.C.A., Lazzeri, A., Vaglini, G., 2015. Improving the analysis of context-aware information via marker-based stigmergy and differential evolution. In *ICAISC 2015, International Conference on Artificial Intelligence and Soft Computing*, Springer LNAI, Vol. 9120, Part II, pp. 1-12.
- Dorigo, M., Bonabeau, E., Theraulaz, G., 2000. Ant algorithms and stigmergy. *Future Generation Computer Systems*, 16(8), 851-871.
- Esling P., Agon, C. Time-series data mining, 2012, *ACM Computing Surveys*, 45(1) 12.
- Fu, T.C., A review on time series data mining, 2011, *Engineering Applications of Artificial Intelligence*, 24, 164-181.
- Lehmann, J., Gonçalves, B., Ramasco, J. J., Cattuto, C., 2012. Dynamical classes of collective attention in twitter. In *WWW 2012, 21st international conference on World Wide Web*, ACM, pp. 251-260.
- Marcus, A., Bernstein, M. S., Badar, O., Karger, D. R., Madden, S., Miller, R. C., 2011. Twitinfo: aggregating and visualizing microblogs for event exploration. In *SIGCHI 2011, conference on Human factors in computing systems*, ACM, pp. 227-236.
- Mohan, C.B., Baskaran, R., 2012. A survey: Ant Colony Optimization based recent research and implementation on several engineering domain. *Expert Systems with Applications*, 39(4), 4618-4627.
- Nichols, J., Mahmud, J., Drews, C., 2012. Summarizing sporting events using twitter. In *IUI 2012, the 2012 ACM international conference on Intelligent User Interfaces*, ACM, pp. 189-198.
- Yun, H. W., 2011. Classifying temporal topics with similar patterns on Twitter. *Journal of information and communication convergence engineering*, 9(3), 295-300.